



Research Article

Non-Hermitian Systems with a Real Spectrum and Selective Skin Effect

Li Ge^{1,2*} 

¹Department of Physics and Astronomy, College of Staten Island, CUNY, Staten Island, NY, USA

²The Graduate Center, CUNY, New York, NY, USA

*Correspondence to: Li Ge, PhD, Professor, Department of Physics and Astronomy, College of Staten Island, CUNY, 10314, USA; Email: li.ge@csi.cuny.edu

Abstract

In this work, we first show a simple approach to constructing non-Hermitian Hamiltonians with a real spectrum, which are *not* obtained by a non-unitary transformation such as the imaginary gauge transformation. They are given, instead, by the product of a Hermitian Hamiltonian H_0 and a positive semi-definite matrix A . Depending on whether A has zero eigenvalue(s), the resulting H can possess an exceptional point at zero energy. When A is only required to be Hermitian instead, the resulting H is pseudo-Hermitian that can have real and complex conjugate energy levels. In the special case where A is diagonal, we compare our approach to an imaginary gauge transformation, which reveals a selective non-Hermitian skin effect in our approach, i.e., only the zero mode is a skin mode and the non-zero modes reside in the bulk. We further show that this selective non-Hermitian skin mode has a much lower lasing threshold than its counterpart in the standard non-Hermitian skin effect with the same spatial profile, when we pump at the boundary where they are localized. The form of our construction can also be found, for example, in dynamical matrices describing coupled frictionless harmonic oscillators with different masses.

Keywords: Non-Hermitian Physics, Parity-Time Symmetry, Non-Hermitian Skin Effect, Topological Lasers

Received: December 30, 2023

Revised: January 16, 2024

Accepted: February 4, 2024

Published: March 15, 2024

Copyright © 2024 The Author(s).

Published by Innovation Forever Publishing Group Limited. This open-access article is licensed under a Creative Commons Attribution 4.0 International License (<https://creativecommons.org/licenses/by/4.0>), which permits unrestricted use, sharing, adaptation, distribution, and reproduction in any medium, provided the original work is properly cited.

Citation: Ge L. Non-Hermitian Systems with a Real Spectrum and Selective Skin Effect. *Innov Discov*, 2024; 1(1): 4.

1 INTRODUCTION

Despite the Hermiticity of quantum mechanics, many quantum and wave systems can be described using a non-Hermitian framework, where a vast subsystem is considered as the reservoir or environment that exchanges particles and energy with the rest of the system. Early investigations of non-Hermitian systems in nuclear physics^[1] employed an open boundary condition of the Schrödinger Equation, which leads to an effectively non-Hermitian Hamiltonian and complex energy levels, with the latter known as resonances or quasi-bound states. Such states correspond to the poles of the scattering matrix, where one or more eigenvalues of the scattering matrix diverge. As such, their presence can be easily detected in the transmission and reflection spectra,

especially when the resonances are close to the real axis. This distance gives the decay rate of a resonance, and it can be compensated by injecting energy into the system, as demonstrated in masers and lasers. For example, one can move a resonance in an optical system to the real frequency axis by providing optical gain, leading to a lasing mode^[2,3].

The combination of these two elements of non-Hermiticity, i.e., loss and gain, can even lead to an entirely real spectrum of a non-Hermitian Hamiltonian, if the complex potential satisfies parity-time (PT) symmetry^[4]. This finding hence raised the possibility of a non-Hermitian extension of standard quantum mechanics. Such PT-symmetric systems can be shown to have pseudo-Hermiticity^[5], meaning that the

Hamiltonian and its Hermitian conjugate are related by a similar transformation. However, just being PT-symmetric or pseudo-Hermitian does not guarantee a real spectrum. In fact, the notion of a spontaneous PT symmetry breaking, signaled by the transition from real eigenvalues to complex conjugate ones, has inspired a cornucopia of findings in photonics and related fields^[6–8], including the enhanced spectral response at an exceptional point (EP)^[9–11]. Unlike a degeneracy in Hermitian systems, an EP is marked by the coalescence of both the energy levels and their wavefunctions. The energy dispersion at an EP usually diverges in some direction(s) of the parameter space, although a perfectly linear dispersion can also be found, e.g., at a Dirac EP^[12,13].

Another approach to constructing a non-Hermitian Hamiltonian with a real spectrum is to perform a non-unitary transformation of a Hermitian Hamiltonian^[14]. Because a similar transformation leaves the spectrum unchanged, this approach guarantees an entirely real energy spectrum, and one can show that this non-Hermitian Hamiltonian is also pseudo-Hermitian. One particular family of transformations within this approach that has generated fast-growing interest is known as an imaginary gauge transformation^[15,16]. This transformation can be understood as replacing the phase in the standard gauge transformation of the Maxwell Equations with its imaginary counterpart, leading to non-reciprocal couplings as well as the superposition of an exponential envelope on all eigenstates of the system. As such, this transformation induces the so-called non-Hermitian skin effect: most (if not all) modes are localized at one side or corner of the system, which has been observed in photonic^[17], acoustic^[18], and mechanical^[19] systems. This effect is not limited to systems in position space with nearest-neighbor couplings and can be extended to synthetic dimensions with longer-range couplings^[12,13].

More generally, a theorem states^[5] that a non-Hermitian Hamiltonian H must be pseudo-Hermitian in order to have a real spectrum, which is proved by assuming a biorthogonal set of eigenstates. This theorem itself, however, does not offer an explicit approach to constructing such a non-Hermitian Hamiltonian, particularly if one wants to go beyond the direct non-unitary transformation mentioned above.

In this article, we first introduce a simple approach that gives non-Hermitian Hamiltonians in their matrix forms with a real spectrum. We start with an arbitrary Hermitian Hamiltonian H_0 , and we show that its product with a positive semi-definite matrix A leads to a non-Hermitian Hamiltonian H with a real spectrum. Because A is arbitrary itself and this procedure is not

a similar transformation, the same H_0 can lead to an infinite set of H 's with different real spectra. Depending on whether A has zero eigenvalue(s), the resulting H can possess an EP at zero energy. When A is only required to be Hermitian instead, the resulting H is pseudo-Hermitian that can have real and complex conjugate energy levels.

In the special case where A is diagonal, we compare our approach to an imaginary gauge transformation, and we show that our approach leads to a selective non-Hermitian skin effect, where only the zero mode is a skin mode and the non-zero modes reside in the bulk. Furthermore, we find that this selective non-Hermitian skin mode has a much lower lasing threshold than its counterpart in the standard non-Hermitian skin effect with the same spatial profile, when we pump at the boundary where they are localized. Finally, we show that the form of our construction can also be found, for example, in non-Hermitian dynamical matrices describing coupled frictionless harmonic oscillators with different masses.

2 MATERIALS AND METHODS

In our analysis below, we perform an eigenvalue analysis of non-Hermitian Hamiltonians and other matrix operators constructed using the method mentioned in the introduction. Default numerical solvers EIG and EIGS in MatLab are used for full and sparse matrices, respectively. The algorithm EIG employs is the QZ or generalized Schur decomposition for a non-Hermitian matrix, while a specialized (and unspecified) algorithm is used by EIGS according to MatLab's documentation. In the discussion of the non-Hermitian skin effect, we adopt a tight-binding model to describe the couplings of a one-dimensional array consisting of microlaser cavities. Threshold analysis is performed to identify the lasing mode with both standard and selective skin effects, which is based on monitoring the complex eigenvalues of the system's Hamiltonian with added optical gain.

3 RESULTS

Below we start our discussion by requiring the matrix A in our construction to be Hermitian but not necessarily positive semi-definite, and we show that the resulting matrix $H=H_0A$ is pseudo-Hermitian that can have either real or pairs of complex conjugate eigenvalues. For this purpose, we first note that H^\dagger is simply given by AH_0 under this condition. Next, if ψ_μ is a right eigenstate of H , we then find

$$H^\dagger(A\psi_\mu) = AH_0(A\psi_\mu) = AH\psi_\mu = \omega_\mu(A\psi_\mu). \quad (1)$$

If $A\psi_\mu=0$, ψ_μ is then an eigenstate of A (and H) with $\omega_\mu=0$ (which is real). If $A\psi_\mu \neq 0$, there is then one left eigenstate $\tilde{\psi}_\nu^\dagger$ of H , defined by $\tilde{\psi}_\nu^\dagger H = \omega_\nu \tilde{\psi}_\nu^\dagger$, or equivalently,

$$H^\dagger \tilde{\psi}_\nu^* = [\tilde{\psi}_\nu^T H]^\dagger = \omega_\nu^* \tilde{\psi}_\nu^*, \quad (2)$$

that satisfies

$$\omega_\mu = \omega_\nu^*, \quad A\psi_\mu = \tilde{\psi}_\nu^*. \quad (3)$$

μ, ν are not necessarily the same, and only when they are does H have a real spectrum. These spectral features indicate that H is pseudo-Hermitian, and if H_0 is invertible, the "metric" η in the definition of pseudo-Hermiticity, i.e., $H^\dagger = \eta H \eta^{-1}$, is simply given by H_0^{-1} :

$$H_0^{-1} H H_0 = H_0^{-1} (H_0 A) H_0 = A H_0 = H^\dagger. \quad (4)$$

Now, if A is not just Hermitian but also positive-definite, we can write A as $B^\dagger B$ where B is an arbitrary square matrix of full rank. We then observe that the biorthogonal inner product

$$\tilde{\psi}_\nu^T \psi_\mu = (\tilde{\psi}_\nu^*)^\dagger \psi_\mu = (A\psi_\mu)^\dagger \psi_\mu = (B\psi_\mu)^\dagger (B\psi_\mu) \geq 0, \quad (5)$$

where we have used the second relation in Equation (3). We note that the equality holds only when $B\psi_\mu = 0$, which contradicts that B is of full rank. Therefore, the inner product $\tilde{\psi}_\nu^T \psi_\mu$ must be finite.

Away from an EP, the biorthogonal relation $\tilde{\psi}_\mu^T \psi_\mu = \delta_{\mu\mu}$ holds. At an EP, its left and right wave functions $\tilde{\psi}_\mu^T, \psi_\mu$ are also "self-orthogonal," i.e., they satisfy $\tilde{\psi}_\mu^T \psi_\mu = 0$, while $\tilde{\psi}_{\mu'}^T \psi_\mu = 0$ still holds when μ' is different from μ . Therefore, if an inner product $\tilde{\psi}_\nu^T \psi_\mu$ is finite, then two conditions must be satisfied: (1) ψ_μ is an eigenstate of H away from an EP, and (2) μ, ν must be the same index. Since the inner product $\tilde{\psi}_\nu^T \psi_\mu$ is finite for any right eigenstate ψ_μ of H , then none of the right eigenstates of H is at an EP, which indicates that H is not defective and has no EPs.

More importantly, with a positive-definite A and $\mu = \nu$, the first relation in Equation (3) then tells us that

$$\omega_\mu = \omega_\mu^* \in \mathbb{R} \quad (6)$$

for all ψ_μ 's, which concludes our proof that all energy levels of H are real and away from an EP when A is positive-definite.

If A is allowed to be positive semi-definite and have zero eigenvalue(s), we can still write $A = B^\dagger B$, but B now has zero eigenvalue(s). As a result, Equation (5) still holds but the equality cannot be eliminated, i.e., with $B\psi_\mu = 0$, and in turn, $A\psi_\mu = 0$, which violates the condition under which Equation (5) is derived. As a result, we find the following properties:

(1) If ψ_μ is an eigenstate of H with a non-zero eigenvalue ω_μ , then $B\psi_\mu \neq 0$, and in turn, we find that ψ_μ is not at an EP and ω_μ is real, similar to the case where A is positive-definite.

(2) Even if ψ_μ is an eigenstate of H with a zero eigenvalue, it is still not at an EP as long as $B\psi_\mu \neq 0$.

(3) ψ_μ can be at an EP only if it is an eigenstate of B (and A, H) with a zero eigenvalue. In other words, H can only have an EP at $\omega_\mu = 0$, with the necessary condition that the corresponding eigenstate ψ_μ satisfies $A\psi_\mu = 0$.

In all our discussions above, the order of A and H_0 in our construction of H is inconsequential; the other order AH_0 gives H^\dagger with the same real eigenvalues.

To understand the conditions leading to the real spectrum of H in our construction, we focus on the special case where A is diagonal and H_0 is given by a tight-binding model:

$$H_0 = \sum_j \omega_j |j\rangle\langle j| + t_{j+1,j} |j+1\rangle\langle j| + t_{j,j+1} |j\rangle\langle j+1|, \quad (7)$$

where ω_j is the on-site potential and $t_{j+1,j}$ is the coupling from lattice site j to $j+1$ and equals the coupling in the opposite direction, i.e., $t_{j,j+1}$. By denoting the diagonal elements of A by a_j 's, we first change the potential landscape, from ω_j 's in H_0 to $a_j \omega_j$'s in H , which does not take place in an imaginary gauge transformation^[21]. Although this procedure maintains the sign of the local potential, it can change a potential barrier to a well and vice versa. At the same time, we also scale the two couplings $t_{j\pm 1,j}$ from site j by the same a_j . This scaling, though, is direction dependent: the pair of couplings $t_{j,j+1}, t_{j+1,j}$ between the two sites $j, j+1$ are scaled by a_{j+1}, a_j , respectively.

As an example, below we consider a one-dimensional system H_0 with a harmonic potential^[22]

$$\omega_j = \left[j - \frac{N-1}{2} \right]^2 \frac{\omega^2}{2} \quad (j = 1, 2, \dots, N; N = 100) \quad (8)$$

(see Figure 1A). The coupling $t \in \mathbb{R}$ is taken to be uniform. For the N eigenstates of H_0 , their lowest energies and corresponding wave functions follow closely the continuous case (see figures 1B and 1C), i.e.,

$$E_q + 2|t| \approx (q - 1/2) \tilde{\omega}, \quad (9)$$

where q is a small positive integer. The offset $2|t|$ is due to the discrete nature of the system, and the effective natural frequency of the harmonic potential is given by $\tilde{\omega} = \omega \sqrt{2|t|}$.

Once we scale ω_j (and t) by an arbitrary $a_j \in (0, 2]$ (see Figure 1A), the spectrum of $H = H_0 A$ is very different and has a much longer tail at both the high and low end of the spectrum (see Figure 1B). Despite the asymmetric couplings in H , the wave functions of its eigenstates are still Anderson localized due to the random scaling we have introduced to the potential, especially the states near the two spectral ends where the spectral density is low (see Figure 1D).

Having exemplified our construction of a non-Hermitian Hamiltonian with a real spectrum, we note that the Hermitian Hamiltonian H_0 in our construction of H cannot be replaced by a non-Hermitian matrix H' with a real spectrum; the resulting $H'' = H'A$ is not even pseudo-Hermitian in general.

One obvious exception is $H' = A^{-1} H_0$ where H_0 is Hermitian, leading to a non-Hermitian $H'' = A^{-1} H_0 A$ with a real spectrum if A is non-unitary. This similar

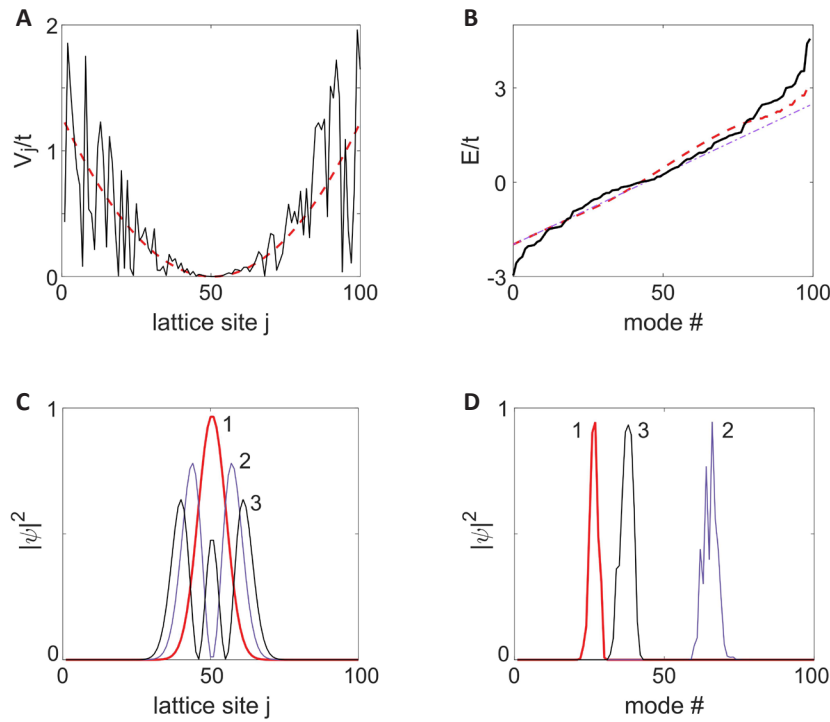


Figure 1. An Example of Constructing a non-Hermitian System with a Real Spectrum. A: Potential in H (solid) and H_0 (dashed). $\omega^2=t/1000$; B: Spectra of H and H_0 , with that of the latter compared with the approximation given by Equation (9) (dash-dotted); C-D: Wave functions of the lowest three energy states in H_0 and H , respectively.

transformation from H_0 to H , with A being diagonal and positive-definite, is the imaginary gauge transformation mentioned previously, which introduces a position-dependent scaling to the eigenstates of H_0 and leads to the non-Hermitian skin effect^[16,17].

The wave functions of H and H_0 in our construction, on the other hand, are not simply related in general, and so are their (real) eigenvalues. This property, as it turns out, leads to a *selective* non-Hermitian skin effect: only the zero mode of the system, i.e., with $\omega_\mu=0$, is exponentially localized at one edge of the system, while the non-zero modes remain in the bulk (Figure 2A). Here the original Hermitian H_0 is given by the tight-binding model (7) with $\omega_j=0$ and $t_{j,j+1}=t_{j+1,j}=t$, and it has chiral symmetry that warrants the zero mode in both the Hermitian case (H_0) and the non-Hermitian cases (H and H'')^[21]. Furthermore, one can show explicitly that the zero modes of $H=H_0A$ and $H''=A^{-1}H_0A$ are exactly the same (Figure 2), but they are formed by different mechanisms as we show below.

The standard non-Hermitian skin effect, as mentioned before, is caused by exponentiating the underlying Hermitian modes via a non-unitary transformation:

$$a_j = s^{j-1}, \quad \psi''_{\mu,j} = \psi_{\mu,j}^{(0)} s^{-(j-1)}, \quad (10)$$

where $j=1, 2, \dots, N$ and $\psi''_{\mu,j}, \psi_{\mu,j}^{(0)}$ are the μ th wave function of H'', H_0 at site j , respectively. The skin modes are localized on the left (right) of the system when $s>1$ ($0<s<1$). The ratio of each pair of (nearest-neighbor) couplings is given by s^2 , and their geometric

average remains unchanged as in H_0 and uniform in space.

For the selective non-Hermitian skin mode in H , its formation is the combination of two effects. One is the same as the standard non-Hermitian skin effect but with the localization length doubled: the ratio of each pair of (nearest-neighbor) couplings is now given by s instead of s^2 , as can be easily checked. In the meanwhile, the geometric average of each pair (i.e., the effective coupling strength) also forms a geometric series, increasing by a factor of s from $\sqrt{t_{j-1,j}t_{j,j-1}}$ to $\sqrt{t_{j,j+1}t_{j+1,j}}$. This increment of the effective coupling strength, similar to the alternate strong and weak couplings in the Su-Schrieffer-Heeger (SSH) array^[23] and the breathing Kagome lattice^[24], contributes the same exponential factor to the wave function as the first mechanism. It then reduces the would-be localization length of the zero mode by half, and we recover the same zero-mode wave function given by Equation (10):

$$\psi_{0,j} = \psi_{0,j}^{(0)} s^{-(j-1)}. \quad (11)$$

We also note that for the corresponding left eigenstate, each pair of couplings $t_{j,j+1}, t_{j+1,j}$ are effectively exchanged, and hence the first mechanism alone would localize the left eigenstate on the right edge of the system instead, similar to what happens in the standard non-Hermitian skin effect (see the dashed line in Figure 2B). The second mechanism mentioned above is not affected by this exchange of $t_{j,j+1}, t_{j+1,j}$, because it is determined only by the geometric average of these two couplings.

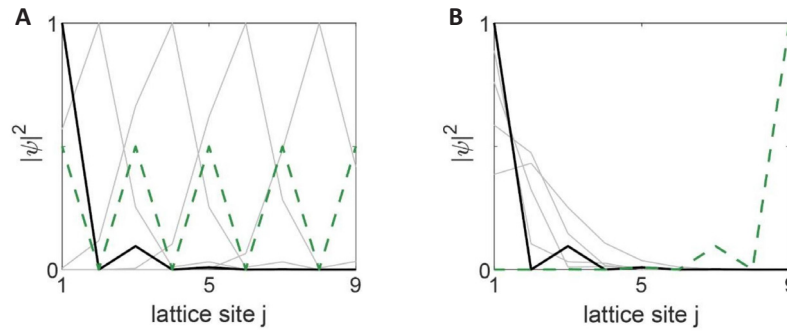


Figure 2. Comparison of Two Different non-Hermitian Skin Effects. A: Selective non-Hermitian skin effect; B: Standard non-Hermitian skin effect. Thick and thin lines show the zero and non-zero modes, respectively. Each thin line represents two modes related by chiral symmetry that have the same spatial profile. Dashed line in each panel shows the left eigenstate of its zero mode.

As a result, acting alone it would still localize the left eigenstate of the zero mode on the left edge of the system, and these two mechanisms hence cancel each other, causing the left eigenstate of the zero mode in the selective skin effect to be extended (see the dashed line in Figure 2A), which has the same spatial profile as the zero mode of the underlying Hermitian Hamiltonian H_0 .

Also due to this increment of the effective coupling, the non-zero modes are now further away spectrally compared to those in H_0 (and H''). In the case shown in Figure 2A, the next two eigenstates of H are at $\omega_{\mu} = \pm 2.38t$, while those in H'' shown in Figure 2B are at $\omega_{\mu} = \pm 0.618t$. Due to such energy differences, the wave functions of non-zero modes in H and H_0 cannot be related directly, and the analysis leading to Equation (11) does not apply to them, indicating the absence of non-Hermitian skin effect in these modes. We also note that the onsite potentials ω_j 's, which are scaled in H from H_0 in general but not in H'' as mentioned previously, do not play a role here because they are all zero.

Another difference between the selective and standard non-Hermitian skin effects is their vastly different lasing thresholds with a localized pump. In this consideration, each site in the tight-binding model represents a laser cavity, and it is typically a micro-ring or micro-disk laser by itself on an integrated photonic platform [25-27]. When the zero mode is the target lasing mode, intuitively one can pump the leftmost cavity in both systems, achieving the lowest lasing threshold by maximizing the spatial overlap between the pump and the zero mode [28].

In the tight-binding model, the radiation and material loss in each cavity are taken into account by making ω_j complex, i.e., adding a negative imaginary part κ_0 . The pump compensates for this loss term by adding a positive imaginary part γ_j , and with spatially uniform pumping, all modes reach their non-interacting lasing threshold simultaneously, given by $\gamma_j = \kappa_0$. Here the non-interacting thresholds ignore the competition for gain among the possible lasing modes, and the lowest one of all modes is the actual lasing threshold with

modal interaction included in this framework, which is a simplified version of the semiclassical laser theory [2,3].

With the selective pumping scenario described above, however, only γ_1 in the leftmost cavity is nonzero, and the threshold of the zero mode is the lowest in both H and H'' . Although the zero mode has the same spatial profile in these two cases, their thresholds still differ significantly. Denoting this zero-mode lasing threshold by D and D'' in these two cases, they are given by $D = 1.44\kappa_0$ and $D'' = 4.99\kappa_0$ when the couplings are much stronger than the cavity loss ($\kappa_0 = 0.02t$).

This difference is caused by the energy exchange between the system and the photonic environment at the coupling junctions [29], which can be quantified by analyzing the dynamical Equation (12) for the intensity in each cavity:

$$\frac{d|\psi_j|^2}{dt} = 2(\gamma_j - \kappa_0)|\psi_j|^2 + \mathcal{P}_{j,j+1} + \mathcal{P}_{j,j-1} \quad (12)$$

where

$$\begin{aligned} \mathcal{P}_{i,i+1} &= it_{i,i+1}^* \psi_{i+1}^* \psi_i + c.c., \\ \mathcal{P}_{j,j-1} &= it_{j,j-1}^* \psi_{j-1}^* \psi_j + c.c. \end{aligned} \quad (13)$$

are the inter-cavity power flows from cavity $j+1$ to j and from cavity $j-1$ to j respectively [29], and *c.c.* stands for the complex conjugation of the first term. This equation indicates that

$$\mathcal{G}_{j,j+1} \equiv \mathcal{P}_{j,j+1} + \mathcal{P}_{j+1,j} = i(t_{j,j+1}^* - t_{j+1,j}) \psi_{j+1}^* \psi_j + c.c. \quad (14)$$

is the power loss (if negative) or gain (if positive) at the coupling junction between cavities j and $j + 1$, which is non-zero only with asymmetric couplings (i.e., $t_{j,j+1}^* \neq t_{j+1,j}$).

Due to the non-Hermitian particle-hole (NHPH) symmetry of both H and H'' [30], the passive zero mode at $\gamma_1 = 0$ becomes a non-Hermitian zero mode [31,32] as γ_1 increases, i.e., without changing its frequency. Its spatial profile, however, is slightly perturbed from that shown in Figure 2, which is no longer "dark" with $\psi_{0,j} = 0$ at the even-numbered lattice sites (Figure 3A). This is another requirement for $\mathcal{G}_{j,j+1}$'s to be non-zero in the zero mode of both H and H'' , and their values

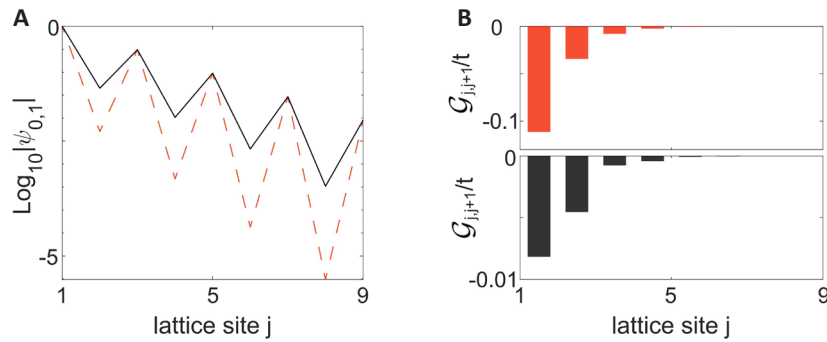


Figure 3. Analysis of the Lasing Mode at Threshold. A: Spatial profile of the zero mode at the lasing threshold in H (solid) and H'' (dashed); B: Its loss to the photonic environment at coupling junctions in H (bottom) and H'' (top). $\mathcal{G}_{j,j+1}$ is centered at $j+1/2$ and with the normalization $\psi_{0,1}=1$ in the leftmost cavity. Here $\kappa_0=0.02t$.

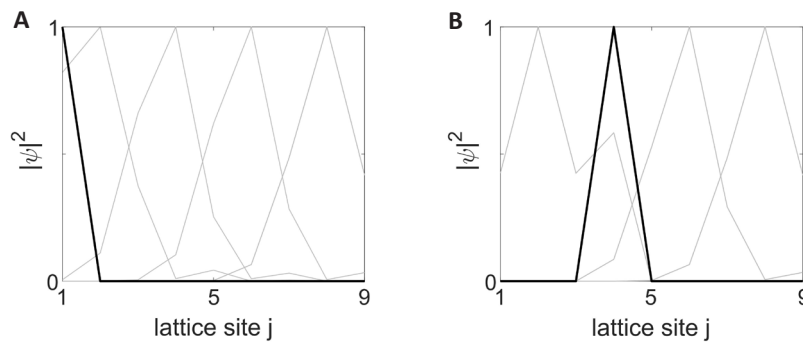


Figure 4. Zero Modes and EP. Both panels are the same as figure 2A, except for A: With $a_1=0$; B: With $a_4=0$. Dashed line in B shows the zero mode at an EP2, while black solid lines in A and B show their zero mode not at an EP.

are shown in Figure 3B. Clearly, $\mathcal{G}_{j,j+1}$'s are all negative in both cases, indicating power loss at the coupling junctions. Furthermore, this power loss is one order of magnitude lower in H than H'' , leading to the much lower threshold in the former. This contrast becomes lower when the couplings are comparable to the cavity loss, e.g., we find $D=1.35\kappa_0$ and $D''=1.62\kappa_0$ when $\kappa_0=t$.

4 DISCUSSION

So far, we have considered examples with a positive-definite A . If A has zero eigenvalue(s) (and is hence positive semi-definite), now H , still possessing a real spectrum, can have an EP at $\omega_\mu=0$ as mentioned previously, if the corresponding eigenstate satisfies $A\psi_\mu=0$.

As an example, we replace a_4 by 0 in the diagonal A used in the case shown in Figure 2A. The resulting H has 6 real and non-zero real energy levels, paired by $\omega_\mu=-\omega_\nu$ due to the chiral symmetry and NHPH symmetry. The other three eigenvalues are zero, but they do not form an EP of order 3. One of them is accompanied by the same selective skin mode ψ_0 given by Equation (11), which is not an eigenstate of the modified A . Therefore, this eigenstate ψ_0 cannot be at an EP of H as we explained earlier, and it forms a single-element Jordan block^[33]. The other two zero eigenvalues form an EP of order 2 (EP2), with the coalesced eigenstate localized at

$j=4$ (Figure 4B). This eigenstate, given by $\psi_{0'}=[0, 0, 0, 1, 0, 0, 0, 0]^T$, indeed satisfies $A\psi_{0'}=0$ as required. The location of this zero mode can be easily understood, because setting $a_4=0$ means that the site $j=4$ does not couple to any other site, and the isolated wave function $\psi_{0'}$ is guaranteed to be a zero mode. The corresponding Jordan chain that completes the Hilbert space can also be found analytically, i.e., $HJ=\psi_{0'}$ with $J=[-1, 0, s^{-2}, 0, 0, 0, 0, 0]^T$. The same outcome holds if we replace another a_j by 0 instead, if j is even.

If this index is odd instead, the outcome becomes very different. For example, if we replace a_1 by 0 instead, then $\omega_\mu=0$ is non-degenerate and not an EP, and the isolated wave function is localized at the left boundary (Figure 4A), replacing the selective skin mode. In this case, the zero-mode wave function $\psi_{0'}=[1, 0, 0, 0, 0, 0, 0, 0]^T$ again satisfies $A\psi_{0'}=0$, but as we mentioned previously, this latter condition is a necessary but not sufficient condition for $\omega_\mu=0$ to be an EP of H .

Furthermore, if N is even instead that deprives H_0 of a zero mode, now replacing one a_j by 0 always gives rise to an EP2, independent of whether j is even or odd (not shown). This zero mode, localized at the j th site, again satisfies $A\psi_{0'}=0$ as required.

Another way to understand these results is the fol-

lowing. With a positive-definite or positive semi-definite A , we write it again as $B^\dagger B$ where B is an arbitrary square matrix. We then find

$$(BH_0B^\dagger)(B\psi_\mu) = \omega_\mu(B\psi_\mu), \quad (15)$$

which means:

If A is positive-definite, then B is of full rank. Therefore, B is invertible and H can be obtained by a similar transformation from the Hermitian Hamiltonian $H_e \equiv BH_0B^\dagger$, i.e.,

$$H = B^{-1}H_eB, \quad (16)$$

indicating that H has an entirely real spectrum. Furthermore, B provides an invertible mapping between the Hilbert spaces of H_e and H , which means every eigenstate φ_μ of H_e is mapped to a distinct eigenstate $\psi_\mu = B^{-1}\varphi_\mu$ of H , ruling out the possibility of having an EP.

When A (and B) is singular with zero eigenvalue(s), every eigenstate ψ_μ of H is mapped to an eigenstate φ_μ of H_e with the same eigenvalue ω_μ , as long as $B\psi_\mu \neq 0$. For a non-zero ω_μ , $B\psi_\mu$ cannot be zero (it leads to $\omega_\mu = 0$), and hence these non-zero ω_μ 's must be real, and so is the entire spectrum of H . At the same time, $H_e\varphi_\mu = \lambda_\mu\varphi_\mu$ leads to

$$(B^\dagger BH_0)(B^\dagger\varphi_\mu) = H^\dagger(B^\dagger\varphi_\mu) = \lambda_\mu(B^\dagger\varphi_\mu), \quad (17)$$

meaning every eigenstate φ_μ of H_e is mapped to an eigenstate of H^\dagger with the same eigenvalue λ_μ as long as $B^\dagger\varphi_\mu \neq 0$. For a non-zero λ_μ , $B^\dagger\varphi_\mu$ cannot be zero (it leads to $\lambda_\mu = 0$). Using these observations and that H, H^\dagger have the same spectrum, we then arrive at the conclusion that the spectra of H and H_e are the same, but one cannot eliminate the possibility that H has EP(s).

As we mentioned in the introduction, our construction of a non-Hermitian H with a real spectrum can also be found in a system of coupled frictionless harmonic oscillators with different masses m_i 's:

$$m_i\ddot{x}_i = -2kx_i + k(x_{i-1} + x_{i+1}). \quad (18)$$

Here \mathbf{x}_i is the displacement of the i th mass, and all masses are connected sequentially by springs with the same spring constant $k \in \mathbb{R}$. If we define the dynamical matrix M as

$$\ddot{\mathbf{x}} = M\mathbf{x} \quad (19)$$

where $\mathbf{x} = [x_1, x_2, \dots, x_N]^T$, then M has the same form AM_0 as in our construction, where A is a diagonal and positive-definite matrix with elements $a_j = m_j^{-1}$ and M_0 is Hermitian and tri-diagonal, with $-2k$ and k on its main diagonal and upper/lower diagonals. Clearly, the system is dissipationless and Hermitian, and hence the harmonic solutions $\mathbf{x}(t) = \mathbf{x}(0)e^{-i\omega_\mu t}$ have real-valued eigenfrequencies ω_μ 's. Consequently, the eigenvalues of M , given by $-\omega_\mu^2$, are all real, despite that M is non-Hermitian if m_i 's are different (e.g., $M_{1,2} = k/m_1 \neq M_{2,1}^* = k/m_2$).

In order to probe a non-Hermitian system with a

real spectrum, typically one shifts the energy of this system such that all energy levels acquire the same imaginary part or linewidth. This linewidth can then be measured either in a passive or active system, which has been done, for example, in PT-symmetric dimers^[6-8]. We expect the same experimental procedure to resolve the real spectrum in our proposed non-Hermitian Hamiltonian, where the reduced lasing threshold of the selective non-Hermitian skin mode can also be verified by comparing it to a system on the same platform with the standard non-Hermitian skin effect^[17]. Such lasers operating in the single or few modes regimes tend to be stable dynamically, thanks to the saturable nonlinearity of the gain medium.

We also stress that even when a non-Hermitian system has a real spectrum, it is our opinion that it should still be considered as a subsystem that exchanges particles and energy with its environment. Therefore, it is expected that the conservation of probability does not hold.

Nevertheless, there are other forms of generalized conservation laws that can be derived in non-Hermitian systems. One simple example is the conservation of probability or optical flux in a one-dimensional system. In a Hermitian system, this conservation law states that $R+T=1$, i.e., the summation of the reflected flux and the transmitted one is conserved. In a non-Hermitian PT-symmetric system, this conservation law evolves to $\sqrt{R_L R_R} = |1 - T|$ ^[34], where T is the still reciprocal transmittance from either the left or right side of the system which can now be larger than 1, while the reflectance from the left R_L and that from the right R_R can be different. In the Hermitian limit, T is always smaller than 1 and $R_R = R_L \equiv R$, and we recover $R+T=1$. Another example is the generalized Ehrenfest theorem defined with respect to a non-Hermitian inner product $(A) \equiv \psi^\dagger A \psi$. When the linear operator A is not explicitly time-dependent, i.e. $(dA/dt)=0$, then it can be shown that (A) is a constant of motion when A defines a pseudo-chirality of the system, i.e., $H^\dagger = -AHA^{-1}$ ^[35].

5 CONCLUSION

In summary, we have presented a systematic approach to constructing non-Hermitian Hamiltonians with a real spectrum beyond a simple similar transformation, which can have embedded EPs at $\omega_\mu=0$ depending on whether A has zero eigenvalue(s). A simple spectral shift can also realize an EP at any desired energy or frequency. Our approach utilizes the product of a Hermitian Hamiltonian H_0 and a positive semi-definite matrix A . Despite bearing similarity to the polar decomposition of an arbitrary square matrix, i.e., as a product of a unitary matrix U and a positive semi-definite matrix A' , here A and A' of H are different: A' is given by $(H^\dagger H)^{1/2} = (AH_0^2 A)^{1/2}$ instead.

The positive semi-definite matrix A does not need to be diagonal, and when it is, we show that our approach can lead to a selective non-Hermitian skin effect, where the zero mode of the system is a skin mode while the non-zero modes still reside in the bulk. We have further shown that the formation of this selective non-Hermitian skin mode is due to two complement mechanisms, i.e., an imaginary gauge transformation and a non-uniform effective coupling strength, each contributing the same exponential factor to the localized spatial profile. Due to the reduced loss to the photonic environment at the non-reciprocal coupling junctions, the lasing threshold of this selective non-Hermitian skin mode is also much lower than its counterpart with the same spatial profile in the standard non-Hermitian skin effect, when we pump at the boundary where they are localized. Our approach may also find applications in constructing and understanding other non-Hermitian matrix operators, including but not limited to the coupled frictionless harmonic oscillators we have discussed.

Acknowledgements

This work is supported by the National Science Foundation (NSF) under Grants No. PHY-1847240 and No. DMR-2326698.

Conflicts of Interest

The author declares no competing interests.

Data Availability

All data generated or analyzed during this study are included in this published article.

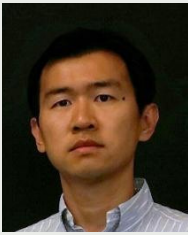
Abbreviation List

PT, Parity-time
EP, Exceptional point
EP2, EP of order 2

References

- [1] Gamow G. Zur quantentheorie des atomkernes. *Z Phys*, 1928; 51: 204-212.[\[DOI\]](#)
- [2] Tureci HE, Ge L, Rotter S et al. Strong interactions in multimode random lasers. *Science*, 2008; 320: 643-646.[\[DOI\]](#)
- [3] Ge L, Chong YD, Stone AD. Steady-state ab initio laser theory: generalizations and analytic results. *Phys Rev A*, 2010; 82: 063824.[\[DOI\]](#)
- [4] Bender CM, Boettcher S. Real spectra in non-Hermitian Hamiltonians having P T symmetry. *Phys Rev Lett*, 1998; 80: 5243.[\[DOI\]](#)
- [5] Mostafazadeh A. Pseudo-Hermiticity versus PT-symmetry. II. A complete characterization of non-Hermitian Hamiltonians with a real spectrum. *J Math Phys*, 2002; 43: 2814-2816.[\[DOI\]](#)
- [6] Feng L, El-Ganainy R, Ge L. Non-Hermitian photonics based on parity-time symmetry. *Nat Photonics*, 2017; 11: 752-762.[\[DOI\]](#)
- [7] Konotop VV, Yang J, Zezyulin DA. Nonlinear waves in PT-symmetric systems. *Rev Mod Phys*, 2016; 88: 035002.[\[DOI\]](#)
- [8] Longhi S. Parity-time symmetry meets photonics: A new twist in non-Hermitian optics. *EPL*, 2018, 120: 64001.[\[DOI\]](#)
- [9] Chen W, Kaya Özdemir Ş, Zhao G et al. Exceptional points enhance sensing in an optical microcavity. *Nature*, 2017, 548: 192-196.[\[DOI\]](#)
- [10] Lai YH, Lu YK, Suh MG, et al. Observation of the exceptional-point-enhanced Sagnac effect. *Nature*, 2019; 576: 65-69.[\[DOI\]](#)
- [11] Hodaie H, Hassan AU, Wittek S, et al. Enhanced sensitivity at higher-order exceptional points. *Nature*, 2017; 54: 187-191.[\[DOI\]](#)
- [12] Rivero JHD, Feng L, Ge L. Imaginary gauge transformation in momentum space and Dirac exceptional point. *Phys Rev Lett*, 2022; 129: 243901.[\[DOI\]](#)
- [13] Rivero JHD, Feng L, Ge L. Analysis of Dirac exceptional points and their isospectral Hermitian counterparts. *Phys Rev B*, 2023; 107: 104106.[\[DOI\]](#)
- [14] Villegas-Martínez BM, Soto-Eguibar F, Hojman SA et al. Non-unitary transformation approach to PT dynamics. arXiv preprint arXiv: 201.06536, 2022.[\[DOI\]](#)
- [15] Hatano N, Nelson DR. Localization transitions in non-Hermitian quantum mechanics. *Phys Rev Lett*, 1996; 77: 570.[\[DOI\]](#)
- [16] Hatano N, Nelson DR. Vortex pinning and non-Hermitian quantum mechanics. *Phys Rev B*, 1997; 56: 8651.[\[DOI\]](#)
- [17] Gao Z, Qiao X, Pan M et al. Two-Dimensional Reconfigurable Non-Hermitian Gauged Laser Array. *Phys Rev Lett*, 2023; 130: 263801.[\[DOI\]](#)
- [18] Zhang X, Tian Y, Jiang JH et al. Observation of higher-order non-Hermitian skin effect. *Nat Commun*, 2021; 12: 5377.[\[DOI\]](#)
- [19] Wang W, Wang X, Ma G. Non-Hermitian morphing of topological modes. *Nature*, 2022; 08: 50-55.[\[DOI\]](#)
- [20] Rivero JHD, Feng L, Ge L. Imaginary gauge transformation in momentum space and Dirac exceptional point. *Phys Rev Lett*, 2022; 129: 243901.[\[DOI\]](#)
- [21] Rivero JHD, Feng L, Ge L. Analysis of Dirac exceptional points and their isospectral Hermitian counterparts. *Phys Rev B*, 2023; 107: 104106.[\[DOI\]](#)
- [22] Leboeuf P, Moulieras S. Superfluid motion of light. *Phys Rev Lett*, 2010; 105: 163904.[\[DOI\]](#)
- [23] Su WP, Schrieffer JR, Heeger AJ. Solitons in polyacetylene. *Phys Rev Lett*, 1979; 42: 1698.
- [24] Ezawa M. Higher-order topological insulators and semimetals on the breathing Kagome and pyrochlore lattices. *Phys Rev Lett*, 2018; 120: 026801.[\[DOI\]](#)
- [25] Chang RK, Campillo AJ. Optical Processes in Microcavities (Advanced Series in Applied Physics). World Scientific: Singapore, 1996.
- [26] Vahala KJ, Optical Microcavities (Advanced Series in Applied Physics). World Scientific: Singapore, 2004.
- [27] Cao H, Wiersig J. Dielectric microcavities: Model systems for wave chaos and non-Hermitian physics. *Rev Mod Phys*, 2015; 87: 61.[\[DOI\]](#)
- [28] Ge L, Gao Z, Feng L. Non-Hermitian gauged laser arrays with localized excitations: Anomalous threshold and generalized principle of selective pumping. *Phys Rev B*, 2023; 108: 104111.[\[DOI\]](#)
- [29] Ge L, Makris KG, Zhang L. Optical fluxes in coupled PT-symmetric photonic structures. *Phys Rev A*, 2017; 96: 023820.[\[DOI\]](#)
- [30] Ge L. Symmetry-protected zero-mode laser with a tunable spatial profile. *Phys Rev A*, 2017; 95: 023812.[\[DOI\]](#)
- [31] Qi B, Zhang L, Ge L. Defect states emerging from a non-Hermitian flatband of photonic zero modes. *Phys Rev Lett*, 2018; 120: 093901.[\[DOI\]](#)
- [32] Ge L. Non-Hermitian lattices with a flat band and polynomial power increase. *Photonics Res*, 2018; 6: A10-A17.[\[DOI\]](#)
- [33] Chen HZ, Liu T, Luan HY et al. Revealing the missing dimension at an exceptional point. *Nat Phys*, 2020; 16: 571-578.[\[DOI\]](#)
- [34] Ge L, Chong YD, Stone AD. Conservation relations and anisotropic transmission resonances in one-dimensional PT-symmetric photonic heterostructures. *Phys Rev A*, 2012; 85: 023802.[\[DOI\]](#)
- [35] Rivero JDH, Ge L. Pseudochirality: a manifestation of Noether's theorem in non-Hermitian systems. *Phys Rev Lett*, 2020; 125: 083902.[\[DOI\]](#)

Brief of Corresponding Author(s)



Li Ge

He received his PhD in Physics from Yale University in 2010, with his thesis focusing on laser physics in complex and disordered media, including wave-chaotic lasers and random lasers. He co-discovered Coherent Perfect Absorbers. Before joining the City University of New York in 2013, professor Ge was a postdoctoral associate in the Department of Electrical Engineering at Princeton University. His current research interests include nonlinear and non-Hermitian phenomena in optics and photonics. Professor Ge has published more than 150 journal articles and conference proceedings in top scientific journals such as *Science*, *Nature*, *Nature Physics*, *Nature Photonics*, and *Physical Review Letters*, with a total citation over 10000 with an h-index of 43.